C. R. Geoscience 342 (2010) 786–795

Contents lists available at ScienceDirect

Comptes Rendus Geoscience

www.sciencedirect.com

Hydrology, environment

Geochemistry, isotopic composition ($\delta^{18}O$, $\delta^{2}H$, $^{87}Sr/^{86}Sr$, $^{143}Nd/^{144}Nd$) in the groundwater of French Guiana as indicators of their origin, interrelations

Géochimie et compositions isotopiques ($\delta^{18}O$, $\delta^{2}H$, $^{87}Sr/^{86}Sr$, $^{143}Nd/^{144}Nd$) des eaux souterraines de Guyane comme indicateurs de leur origine et interrelations

Philippe Négrel *, Emmanuelle Petelet-Giraud

BRGM, avenue Claude-Guillemin, BP 6009, 45060 Orléans cedex 02, France

ARTICLE INFO

Article history:
Received 14 April 2010
Accepted after revision 27 July 2010

Presented by Ghislain de Marsily

Keywords:
French Guiana
Groundwater
Strontium isotopes
Neodymium isotopes

ABSTRACT

The current use of untreated river water for drinking purposes by the population of French Guiana has important impacts on public health. Consequently, groundwater is of major importance as a possible alternative drinking water supply to reduce these impacts. Since French Guiana belongs to the Guyana Shield, sustainable water management can be expected to depend increasingly on water from fissured aquifers in hard rocks. Groundwater samples were collected from shallow drill holes in the densely populated coastal area, and deeper wells in the basement (around Cayenne and along the Maroni and Oyapock rivers). This study reports on major and trace elements for which Na^{+} and Ca^{2+} excess with regard to Cl reflect the role of water-rock interaction, as well as Sr and Nd isotopes that reflect the role of the different lithologies. $\delta^{18}O$ and δD in waters give constraints on the water cycle (recharge and evaporation processes).

Mots clés :
Guyane française
Eau souterraine
Isotopes du strontium
Isotopes du néodyme

RÉSUMÉ

L'utilisation d'eau de surface non traitée comme eau de boisson par la population guyanaise a des effets importants en termes de santé publique. En conséquence, les ressources en eaux souterraines sont d'une importance majeure comme alternative pour l'alimentation en eau potable, afin de réduire les impacts sur la santé publique. La Guyane française faisant partie du bouclier guyanais, les ressources en eau souterraine sont probablement contenues dans les roches fracturées. Des eaux souterraines ont été prélevées dans des forages peu profonds dans les zones de forte densité de population dans la zone côtière et dans des ouvrages plus profonds dans les zones de socle (proche de Cayenne et le long des fleuves Maroni et Oyapock). Cette étude présente la géochimie des éléments majeurs et traces pour lesquels les excès de Na^{+} et Ca^{2+} par rapport au Cl reflètent le rôle des interactions eau-roche, tandis que les isotopes du Sr et Nd montrent le rôle des différentes lithologies drainées. Les isotopes de la molécule d'eau ($\delta^{18}O$ et δD) tracent le cycle de l'eau, précisant la recharge et les processus d'évaporation.

* Corresponding author.
E-mail addresses: p.negrel@brgm.fr (P. Négrel), epetelet@brgm.fr (E. Petelet-Giraud).

1631-0713/$ – see front matter
doi:10.1016/j.crte.2010.07.003

1. Introduction

Groundwater resources are of the utmost importance in French Guiana for water supply because the use of untreated river water for drinking by the inland population induces important health impacts. Since French Guiana belongs to the Guyana Shield, sustainable water management can be expected to depend increasingly on water from fissured aquifers, e.g. mainly hard rocks (crystalline, metamorphic and volcanic rocks). The exploitation of such fissured (heterogeneous and anisotropic) systems has to be linked to the characterisation of aquifer structure and functioning, aquifer heterogeneities and relationships with surface water (Négrel and Lachassagne, 2000; Négrel et al., 2002).

Present-day research has to focus on increasing use of existing geochemical tools (such as Sr-Nd isotopes as well as lead isotopes) dedicated to elucidate the structure and functioning of the different compartments of hard rock aquifers, i.e. overlying sediments, when they do exist, weathered cover alterites, weathered-fissured zone, fractured hard rock (Négrel, 2006; Steinmann and Stille, 2006). In particular, research will have to deal with the identification of the relative signature of groundwater circulations in the alterites and in the underlying weathered-fissured zone. This zone, with efficient porosities ranging from 3 to 20% in the alterites and from 0.5 to 2% in the weathered-fissured zone, may contain most of the groundwater reserve (since the efficient porosity of fresh bedrock is often less than 0.01%). This will also help to identify the role of these different hydrogeological compartments, both under natural and pumping conditions, and in the framework of surface-groundwater relationships. These methods give better understanding of the alterites and underlying weathered-fissured zone as hydrogeophysics, e.g. use of advanced geophysical methods to understand the interaction between geology and fluid flow in the subsurface, did (Auken et al., 2009; Sailhac et al., 2009).

Since a sufficient number of boreholes have been drilled in French Guiana (Fig. 1), ongoing research is now focusing on the geochemistry of ground waters for which the database will serve to build up a referential for this region and will be valorised in conjunction with geologic, hydrodynamic, etc., data, as one main objective will be to better define the functioning of French Guiana hard rock aquifers.

2. General conditions in French Guiana

French Guiana covers 10% of the Guyana Shield, which represents the northern extension of the Amazonian Platform (Deckart et al., 2005; Edmond et al., 1995). The Guyana Shield comprises three rock complexes: the Imataca Archaen gneiss (3.4–2.7 Ga), the Lower Proterozoic volcano-sedimentary terrains and granite-gneiss rocks (2.3–1.9 Ga), and the Middle Proterozoic continental deposits and magmatic rocks (1.9–1.5 Ga). With regard to its weathered substratum, which is composed only of Lower Proterozoic (2.5–1.9 Ga) igneous and metamorphic rocks, French Guiana is similar to the Guyana Shield

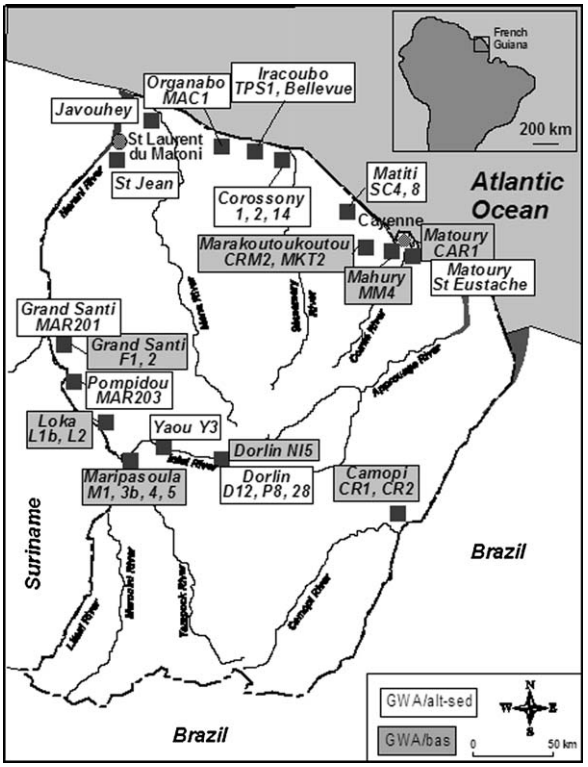

Fig. 1. Map showing the site locations in French Guiana where groundwaters were sampled and analysed for major ions and isotope systematics.

Fig. 1. Carte de localisation des sites d'échantillonage des eaux souterraines en Guyane pour analyses des ions majeurs et des isotopes.

drained by the Orinoco (Edmond et al., 1995). The geology of French Guiana can be summarized as four different units (Deckart et al., 2005; Gruau et al., 1985) with the Cayenne Island series, the Lower Paramaca (hereafter referred to as unit P) of mainly metavolcanic rocks and rare sediments, the Upper Paramaca (hereafter referred to as unit S) and Orapu comprising schists, micaschists, quartzites, conglomerates, metagraywackes, metasiltites and rare metavolcanic rocks and finally plutonic intrusions of gabbro-diorite, granite and granodiorite from the "Guyana plutonism", and granitoid, granodiorite and tonalite from the "Caribbean plutonism".

The climatic and geodynamic conditions over the Guyana Shield since the Cretaceous have induced the extensive development of 50 to 100 m thick alterites masking the substratum (Driscoll and Karner, 1994). The climate is humid tropical, with two rainy seasons and two dry seasons and the total annual effective rainfall is around 1000 mm/year. Most of the groundwater resource is located in the crystalline bedrock, typical of those of tropical hard rock settings. The alluvia have high clay content, mainly due to the nature of the sediments in tropical settings and also due to local weathering, they are relatively thin (mainly less than 5 m) and are of reduced lateral extent; they, therefore, account for only a small volume of groundwater. The alterites, which constitute the upper compartment of the bedrock aquifers, have an

effective porosity of a few percent and, thus, a water storage function.

3. Sampling procedures and analytical methods

Groundwater samples (Fig. 1) were collected:

- along the coastal area bordering the Atlantic Ocean from shallow drill holes in the extensive sandy-argillaceous terrane, mainly Holocene in age, (GWA/alt-sed in Table 1), which is the only densely populated area in French Guiana (Négrel et al., 2002);
- along the Maroni and Oyapock River catchments (Négrel and Lachassagne, 2000) from shallow wells in the alluvia (GWA/alt-sed in Table 1).

Groundwater samples were also collected from deep wells in the basement (Fig. 1), MM4, CAR1 and MKT2 around Cayenne (GWA/bas in Table 1) from which groundwater is pumped from bedrock fractures, deep wells (GWA/bas in Table 1) in the basement along the two main rivers Maroni and Oyapock (F1, 2, M1, 3bis, 4, 5, L1bis, 2, CR1, 2) and more inland (Ni5).

Groundwater were filtered on site through 0.2 μm acetate cellulose filters and stored in pre-cleaned polypropylene bottles. The samples for cation and isotope measurements were acidified to pH 2 with ultrapure HNO_3, and one bottle of each sample (not acidified) was kept for anion determination. Electrical conductivity, water temperature and pH were measured in the field with a conductivity meter standardized to 20 °C and with a combined electrode and a pH-meter regularly calibrated using two standard buffers. Chemical analysis of the water samples was carried out by capillary ion electrophoresis for major cations and anions, by ICP-MS for Sr, Sm and Nd and HCl titration and Gran's method for the total alkalinity. Precision ranged between ±5 and 10% for the determination of major and trace elements measurements. Classical methods for the separation by exchange column (cation for Sr, cation and HDEHP reverse chromatography for Nd) and isotope analysis (Finnigan MAT 262 multiple collector mass spectrometer) were used for Sr and Nd isotope

Table 1
Groundwater typology, well type and lithology in the extensive sandy-argillaceous terrane from the coastal area and from shallow wells in the alluvia along the Maroni and Oyapock River catchments (GWA/alt-sed) and from deep wells in the basement (GWA/bas).

Tableau 1
Typologie des eaux souterraines, type d'ouvrage et lithologie dans la zone argilo-sableuse de la zone côtière et des aquifères superficiels des bassins versants du Maroni et de l'Oyapock (GWA/alt-sed) et des ouvrages profonds dans la zone de socle (GWA/bas).

Name	Type	Reference	Well type	Lithology
Grand Santi	GWA/alt-sed	MAR201	Well in the village (5 m)	Sand, clays, alluvial deposits
Pompidou	GWA/alt-sed	MAR203	Well in the village (5 m)	Sand, clays, alluvial deposits
Grand Santi	GWA/alt-sed	MAR201	Well in the village (5 m)	Sand, clays, alluvial deposits
Yaou 3	GWA/alt-sed	Y 3	Spring from saprolite	Meta-volcanic rocks (basalt, amphibolite) Lower Paramaca P
Dorlin 14	GWA/alt-sed	D14	Spring from saprolite	Meta-volcanic rocks (basalt, amphibolite) Lower Paramaca P
Inini	GWA/alt-sed	25	Spring	Sand, clays, alluvial deposits
Inini	GWA/alt-sed	P8	Shallow drill hole (2 m)	Sand, clays, alluvial deposits
St Eustache	GWA/alt-sed	GUY99-03	Spring from saprolite	Granitoide, migmatites, Caribbean plutonism γ
Corossony 1	GWA/alt-sed	GUY99-04	Piezometer (10 m)	Sand, clays developped on granitoides Caribbean plutonism γ
Corossony 2	GWA/alt-sed	GUY99-05	Piezometer (10 m)	Sand, clays developped on granitoides Caribbean plutonism γ
Corossony 14	GWA/alt-sed	GUY99-06	Piezometer (10 m)	Sand, clays developped on granitoides Caribbean plutonism γ
TPS1	GWA/alt-sed	GUY99-07	Drill hole (20 m)	Sand, clays developped on granitoides Caribbean plutonism γ
Bellevue	GWA/alt-sed	GUY99-08	Drill hole (20 m)	Sand, clays developped on granitoides Caribbean plutonism γ
MAC1	GWA/alt-sed	GUY99-09	Drill hole (20 m)	Sand, clays developped on granitoides Caribbean plutonism γ
St Jean	GWA/alt-sed	GUY99-10	Well in the village (5 m)	Sand, clays, alluvial deposits
Javouhey	GWA/alt-sed	GUY99-11	Drill hole	Sand, clays, littoral deposits
SC8	GWA/alt-sed	GUY99-12	Drill hole (20 m)	Sand, clays, littoral deposits
SC4	GWA/alt-sed	GUY99-13	Drill hole (20 m)	Sand, clays, littoral deposits
Camopi	GWA/bas	CR1	Drill hole (30 m)	Migmatites
Camopi	GWA/bas	CR2	Drill hole (20 m)	Migmatites
Grand Santi	GWA/bas	F1	Drill hole (50 m)	Migmatites
Grand Santi	GWA/bas	F2	Drill hole (60 m)	Migmatites
Grand Santi	GWA/bas	F1/1 h	Drill hole (50 m)	Migmatites
Grand Santi	GWA/bas	F1/72 h	Drill hole (50 m)	Migmatites
Grand Santi	GWA/bas	F2/72 h	Drill hole (60 m)	Migmatites
Grand Santi	GWA/bas	F1	Drill hole (50 m)	Migmatites
Grand Santi	GWA/bas	F2	Drill hole (60 m)	Migmatites
Maripasoula	GWA/bas	M1	Drill hole (70 m)	Meta-volcanic rocks (basalt, amphibolite) Lower Paramaca P
Maripasoula	GWA/bas	M3 bis	Drill hole (65 m)	Meta-volcanic rocks (basalt, amphibolite) Lower Paramaca P
Maripasoula	GWA/bas	M4	Drill hole (60 m)	Meta-volcanic rocks (basalt, amphibolite) Lower Paramaca P
Maripasoula	GWA/bas	M5	Drill hole (75 m)	Meta-volcanic rocks (basalt, amphibolite) Lower Paramaca P
Loka	GWA/bas	L1 bis	Drill hole (50 m)	Meta-volcanic rocks (basalt, amphibolite) Lower Paramaca P
Loka	GWA/bas	L2	Drill hole (50 m)	Meta-volcanic rocks (basalt, amphibolite) Lower Paramaca P
Dorlin	GWA/bas	Ni 5	Artesian drill hole (1 m^3/h)	Meta-volcanic rocks (basalt, amphibolite) Lower Paramaca P
Marakoutoukoutou	GWA/bas	CRM2	Drill hole (90 m)	Granitoide, Caribbean plutonism
MM4	GWA/bas	GUY99-01	Drill hole (100 m)	Diorites
CAR1	GWA/bas	GUY99-02	Drill hole (80 m)	Leptyno-amphibolite Ile de Cayenne series
Marakoutoukoutou	GWA/bas	MKT2	Drill hole (100 m)	Granitoide, Caribbean plutonism

Table 2
Major field parameters, major and trace elements, and isotopic data ($^{87}Sr/^{86}Sr$, $\delta^{18}O$, $\delta^{2}H$ and εNd(0)) in the groundwaters of French Guiana.

Tableau 2
Paramètres de terrain, éléments majeurs et traces et données isotopiques ($^{87}Sr/^{86}Sr$, $\delta^{18}O$, $\delta^{2}H$ et εNd(0)) dans les eaux souterraines de Guyane.

Name	Type	Reference	EC	T	pH	Ca	Na	Mg	K	Cl	SO_4	NO_3	HCO_3	Sr	$^{87}Sr/^{86}Sr$	Eps Nd (0)	$^{147}Sm/^{144}Nd$	Nd	Sm	$\delta^{2}H$	$\delta^{18}O$
			μS/cm	°C						μmol/l								ng/l	ng/l		
Grand Santi	GWA/alt-sed	MAR201	39.5	28.5	5.8	85	170	21	13	70	2	10	391	0.321	0.708130	–	–	–	–	−15.7	−3.5
Pompidou	GWA/alt-sed	MAR203	46.4	19.7	5.99	65	248	8	21	180	2	31	200	0.142	0.710147	–	–	–	–	−16.8	−3.3
Grand Santi	GWA/alt-sed	MAR201	46.4	27.8	5	100	152	33	49	149	3	119	300	0.571	–	–	–	–	−16.6	−3.4	
Yaou 3	GWA/alt-sed	Y 3	58	24.3	6.05	78	109	177	24	67.6	14	*dl*	505	0.231	0.708453	–	–	–	–	−14.5	−3.3
Dorlin14	GWA/alt-sed	D14	44	23.6	6.94	62	142	116	27	185.9	35	2	205	0.120	0.710646	–	–	–	–	−15.3	−3.3
Inini	GWA/alt-sed	25	40.7	25.6	5.4	10	157	58	10	197	32	6	38	0.033	0.713692	–	–	–	–	−19.2	−3.7
Inini	GWA/alt-sed	P8	21.1	30.7	5.13	5	109	8	13	99	7	3	19	0.021	0.709707	–	–	–	–	−14.3	−2.8
St Eustache	GWA/alt-sed	GUY99-03	39	25.7	4.48	20	175	40	12	185	12	28	–	0.029	0.728571	−12.64	0.1342	123	27.3	−12.4	−3.2
Corossony 1	GWA/alt-sed	GUY99-04	113	33.3	6.19	67	396	86	44	254	9	4	770	0.342	0.709466	−12.00	0.1209	130	26	−10.7	−2.4
Corossony 2	GWA/alt-sed	GUY99-05	67	30.3	5.19	16	2009	49	35	4241	10	*dl*	210	0.072	0.709461	−10.42	0.1321	65	14.2	−7.9	−2.1
Corossony 14	GWA/alt-sed	GUY99-06	298	29.8	7	228	9468	457	95	10174	70	*dl*	2680	1.335	0.708714	−11.63	0.1205	134	26.7	−14.4	−3.2
TPS1	GWA/alt-sed	GUY99-07	84	27.7	5.63	34	273	112	58	276	25	*dl*	410	0.215	0.721651	−13.28	0.1358	297	66.7	−14.7	−3.1
Bellevue	GWA/alt-sed	GUY99-08	27	26.7	4.53	10	123	28	16	106	5	10	150	0.042	0.713712	−11.22	0.1354	39	8.7	−12.6	−3
MAC1	GWA/alt-sed	GUY99-09	23	29.2	4.4	10	95	18	9	51	4	3	70	0.027	0.710370	−17.83	0.1048	96	16.7	−14.1	−3.1
St Jean	GWA/alt-sed	GUY99-10	98	26.2	6.31	235	243	50	104	120	21	*dl*	740	0.566	0.717093	–	–	–	–	−9.9	−2.5
Javouhey	GWA/alt-sed	GUY99-11	166	28.5	6.56	717	106	46	39	175	3	84	1310	0.284	0.707984	−14.71	0.0858	60	8.6	−11.3	−2.8
SC8	GWA/alt-sed	GUY99-12	281	29.4	6.64	139	1886	280	96	457	14	*dl*	2160	0.612	0.709211	−10.59	0.1182	752	147	−14.4	−3.3
SC4	GWA/alt-sed	GUY99-13	39	29	5.01	23	150	35	23	154	9	*dl*	110	0.059	0.713286	−9.25	0.1446	62	14.8	−9.7	−2.5
Camopi	GWA/bas	CR1	–	–	–	28	122	33	33	56	5	18	*200*	0.134	0.723978	–	–	–	–	−12.3	−2.9
Camopi	GWA/bas	CR2	–	–	–	25	109	25	26	59	5	19	*150*	0.134	0.725469	–	–	–	–	−12.7	−3.1
Grand Santi	GWA/bas	F1	146.9	26.4	6.6	475	365	188	18	45	1	*dl*	*1750*	1.027	–	–	0.1172	4	0.9	−16.4	−3.6
Grand Santi	GWA/bas	F2	198.5	26.2	6.93	783	465	208	21	54	7	*dl*	*2200*	1.484	–	–	0.1587	8	2.0	−17.8	−3.6
Grand Santi	GWA/bas	F1/1h	181	27.1	6.88	403	426	200	–	59	4	*dl*	1754	0.913	0.704100	–	–	–	–	–	–
Grand Santi	GWA/bas	F1/72h	148	26.9	6.38	535	478	254	–	62	6	*dl*	2197	1.142	0.704200	–	–	–	–	–	–
Grand Santi	GWA/bas	F2/72h	196	26.5	6.83	600	474	225	–	70	7	*dl*	2295	1.142	0.703985	–	–	–	–	–	–
Grand Santi	GWA/bas	F1	176	–	7.16	674	140	189	19	50.7	20	*dl*	1767	1.244	0.705429	−18.82	0.1512	3	0.7	–	–
Grand Santi	GWA/bas	F2	215	–	6.95	668	445	238	32	84.5	11	2	2231	1.507	0.704584	–	–	–	–	–	–
Maripasoula	GWA/bas	M1	–	–	–	341	581	190	23	84.5	13	*dl*	1539	1.758	0.703520	–	0.1109	9	1.7	–	–
Maripasoula	GWA/bas	M3 bis	–	–	–	498	410	597	18	59.2	9	*dl*	2543	2.055	0.704046	–	0.0807	18	2.4	–	–
Maripasoula	GWA/bas	M4	–	–	–	772	476	498	20	56.3	10	2	2979	3.174	0.703624	–	0.0676	8	0.9	–	–
Maripasoula	GWA/bas	M5	–	–	–	317	372	377	28	107.0	6	15	1708	1.689	0.703596	–	0.0850	25	3.5	–	–
Loka	GWA/bas	L1 bis	–	–	–	796	294	288	12	59.2	8	*dl*	2354	1.975	0.704260	−15.33	0.1257	8	1.6	–	–
Loka	GWA/bas	L2	–	–	–	999	329	310	29	56.3	11	*dl*	2877	2.192	0.705883	–	0.1076	19	3.3	–	–
Dorlin	GWA/bas	Ni 5	186	24.9	6.22	290	245	415	22	270.4	87	3	1302	2.295	0.704149	–	0.0430	34	2.4	−18.4	−3.7
Marakoutoukoutou	GWA/bas	CRM2	62	–	5.58	88	230	45	19	157	17	64	415	0.459	0.713903	–	–	–	–	−12.7	−3.1
MM4	GWA/bas	GUY99-01	275	26.6	7.18	766	693	312	49	151	32	5	2560	1.507	0.713512	−15.16	0.1348	5	1.1	−17.9	−4
CAR1	GWA/bas	GUY99-02	156	26	6.14	272	471	264	93	149	23	*dl*	1330	1.666	0.709933	−24.56	0.0890	6	0.8	−15.9	−3.7
Marakoutoukoutou	GWA/bas	MKT2	237	25.6	6.62	518	952	175	82	408	89	2	1885	1.723	0.712861	–	–	–	–	−13.4	−3.2

measurements (Négrel and Lachassagne, 2000; Négrel et al., 1997). The reproducibility of $^{87}Sr/^{86}Sr$ measurement was tested by duplicate analyses of the NBS 987 standard (mean value $0.710227 \pm 17 \times 10^{-6}$, 2σ, $n = 70$) of the La Jolla international standard for Nd ($^{143}Nd/^{144}Nd$ of $0.511826 \pm 11 \times 10^{-6}$, 2σ, $n = 33$). The $^{143}Nd/^{144}Nd$ ratios are expressed as εNd(0), which represents the deviation in parts per 10^4 (ε unit) from $^{143}Nd/^{144}Nd$ in a chondritic reservoir with a present day CHUR value of 0.512636. Data are presented in Table 2.

4. Results and discussion

4.1. Chemical characterisation of waters

The Total Dissolved Solids (TDS) fluctuates from 10 up to 166 mg/L in the groundwater from the extensive sandy-argillaceous terrane and from the alluvia (hereafter referred to as GWA/alt-sed) and from 46 to 218 mg/L in the groundwater from the basement (hereafter referred to as GWA/bas). The water chemistry shows a large variation in major element contents (Table 2). Chloride content in the GWA/alt-sed groundwater ranges from 50 to 4241 μmol/L and from 45 to 457 μmol/L in the GWA/bas groundwater. Though Cl^- ions do not have any significant lithological origin, since French Guiana is evaporite free, Cl^- ions in groundwater may originate mainly from rainfall recharge (sea salts, Gaillardet et al., 1997), and to a lesser extent from human activity (domestic sewage, fertilisers, etc). Chloride often behaves conservatively through the hydrological cycle and is used as an atmospheric-input reference element in many hydrosystems (Gaillardet et al., 1997). Like Cl^-, Na^+ shows a wide range of contents and, when compared to Cl^- in Fig. 2a, Na concentrations in most surface and ground waters plot above the seawater dilution line (SWDL), indicating Na^+ excess. Most of the surface and ground waters from the GWA/alt-sed plot between the SWDL and the line have a molar Cl/Na ratio of around 0.5. Three GWA/bas ground waters (CR1, CR2 and F1-oct-98) plot with a molar Cl/Na ratio of 0.7, the hydrogeological data suggest that the alterite compartment contributes significantly to the well flow rate. The remaining GWA/bas ground waters plot with a molar Cl/Na ratio of 0.2. This divergence from the seawater dilution line reflects a large Na enrichment that is mainly related to water-rock interaction. Ca^{2+} concentrations show a large range in groundwater from about 5–10 to 999 μmol/L and fluctuate also largely in rain and surface waters when compared to Cl^- in Fig. 2b (all samples plot above the SWDL, with a Cl/Ca ratio of 1.42 for the surface waters indicative of a Ca^{2+} excess). The groundwater from the GWA/alt-sed also display a Ca^{2+} excess and plot with a molar Cl/Ca ratio ranging between that of SWDL and the ratio 1.42, four of them plot with a molar Cl/Ca ratio higher than 1.42. The GWA/bas groundwater plot with a molar Cl/Ca ratio ranging between 1.42 and 0.05, reflecting the larger Ca^{2+} excess. Some of them plot with a molar Cl/Ca ratio of around 1.42, close to the groundwater from the GWA/alt-sed, reflecting the fact that water partly originates from the alterite compartment. Similarly, K^+, Mg^{2+} and Sr^{2+} excess are observed when plotted versus Cl^-, (not shown), reflecting the weathering of aluminosilicates.

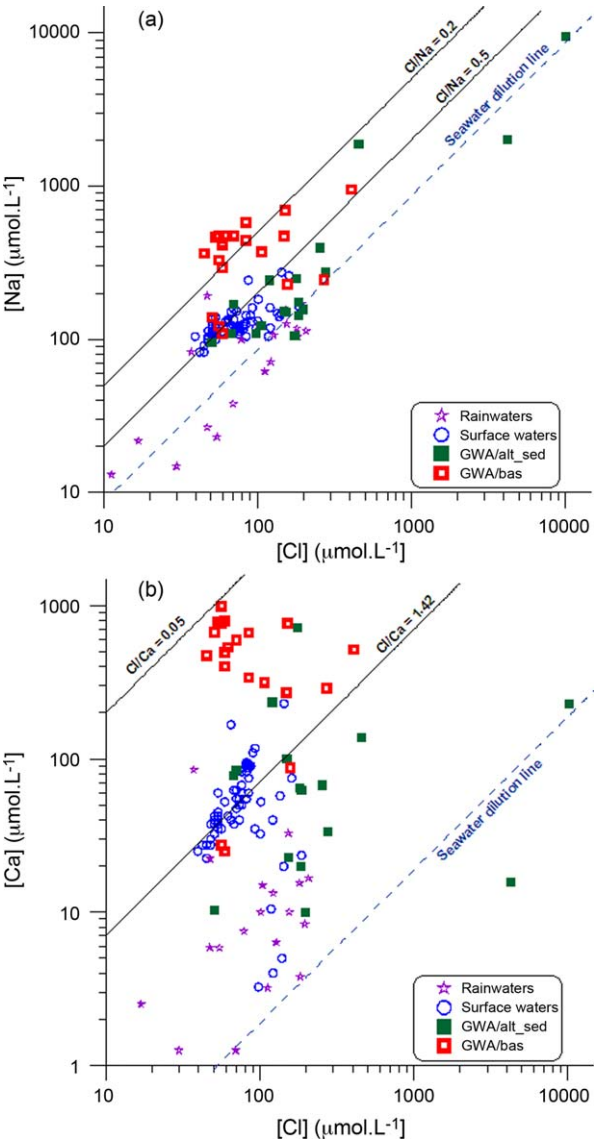

Fig. 2. (a) Cl vs Na concentrations (in μmol/l) in surface- and groundwaters from French Guiana; (b) Cl vs Ca concentrations (in μmol/l) in surface- and groundwaters from French Guiana. Rainwater data are from Négrel et al. (1997) and surface water data are from Négrel and Lachassagne (2000).

Fig. 2. (a) Concentrations des eaux de surface et souterraines de Guyane en Cl et Na (en μmol/l); (b) Cl vs Ca (en μmol/l) dans les eaux de surface et souterraines de Guyane. Les données des eaux de pluie sont extraites de Négrel et al. (1997); celles des eaux de surface sont extraites de Négrel et Lachassagne (2000).

The positive correlation between HCO_3 and the sum of cations in groundwater samples (Σ^+, $r^2 = 0.55$, $n = 38$) clearly indicates that the cations released by weathering are balanced by the alkalinity, in good agreement with observations in other South American basins influenced by similar climatic conditions (Freyssinet and Farah, 2000;

Gaillardet et al., 1997). The bicarbonate increase during weathering originates from the atmospheric/soil CO_2, which implies a positive correlation between HCO_3 and pH in groundwater samples ($r^2 = 0.66$, $n = 38$) related to the water-rock interaction.

4.2. Investigating groundwater recharge through δ^2H and $\delta^{18}O$ isotopic signature

Variations in the stable-isotope composition in a catchment's water balance are mainly caused by natural variations in the isotopic composition of rainfall and through mixing with pre-existing water and the influence of evaporation (Kendall and McDonnell, 1998). The stable isotopes δ^2H and $\delta^{18}O$ of all rain samples collected in French Guiana (Négrel et al., 1997) define the local meteoric water line (LMWL), as illustrated in Fig. 3a. The $\delta^{18}O$ and δ^2H in GWA/alt-sed ground waters fall in the range −2.1 to −3.7‰ for $\delta^{18}O$ and −7.9 to −19.2‰ for δ^2H and in the range −2.9 to −4.0‰ for $\delta^{18}O$ and −12.3 to −18.4‰ for δ^2H for the GWA/bas ground waters, in close agreement with the range of surface water (Négrel and Lachassagne, 2000).

The $\delta^{18}O$ and δ^2H relationships are illustrated in Figs. 3a and b for rainwater (regression line and 95% confidence range), global meteoric water line (GMWL; $\delta^2H = 8\ \delta^{18}O + 10$, Craig, 1961), surface waters and groundwater. Surface waters plot close to the LMWL in Fig. 3b and, as demonstrated by Négrel and Lachassagne (2000), most show a significant shift (close to 1.4‰) to the right of this line as result of evaporation processes. Most of the ground waters from GWA/alt-sed clearly plot close to the local and global lines. Some of these ground waters are displaced below the LMWL. This could be due either to evaporation prior or during infiltration or, as suggested by Boronina et al. (2005), because of partial evaporation from soils and dilution by subsequent recharge. GWA/bas groundwater also plot close to the LMWL and GMWL, reflecting a meteoric origin and a lack of significant evaporation during recharge or oxygen isotope exchanges between water and the rock matrix.

Infiltrating rainwater shows a mean weighted signatures for $\delta^{18}O$ and δ^2H of −4.51 and −24.23‰ respectively, corresponding to 1790.4 mm of rainfall (Négrel et al., 1997). However, mean rainwater δ-values cannot explain groundwater recharge as less negative values occur in many samples (Fig. 3b). Thus, recharge from precipitation events occurs in significant amount at least during two periods. The first period was September to January and corresponds to the rainy season with 496 mm of rainfall (27.7% of the total annual rainfall, mean weighted rain signatures input led to $\delta^{18}O$ and δ^2H of around −2.45 and −7.58‰, respectively). The second period occurred in March-April with 249 mm rainfall, which corresponds to the middle of the rainy season (13.9% of the total annual rainfall, mean weighted rain input led to $\delta^{18}O$ and δ^2H signatures of around −3.10 and −11.11‰, respectively). These two rainy periods should constitute the recharge period that would explain the least negative δ-values in the ground waters. It is worth noting that part of the $\delta^{18}O$ and δ^2H signatures in the groundwater should reflect the

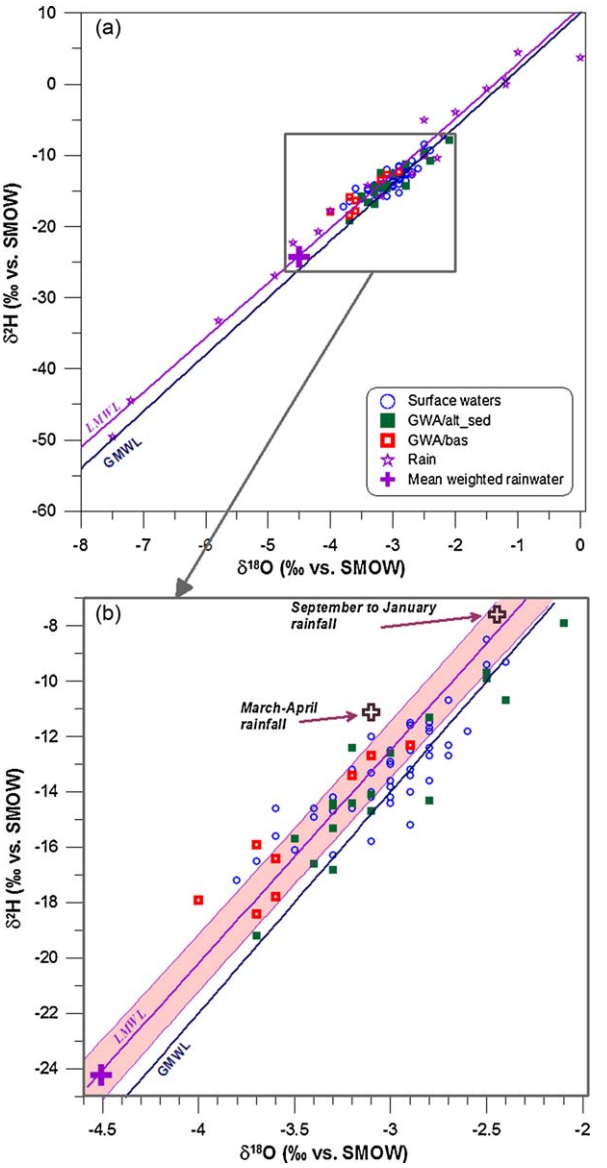

Fig. 3. Relationships between δ^2H and $\delta^{18}O$ (‰ vs SMOW Standard Mean Ocean Water) in surface- and groundwaters collected from French Guiana (a). Rainwater data, e.g. Local Meteoric Water Line LMWL, i.e. 10 monthly accumulations and 3 individual rain events in Cayenne (Négrel et al., 1997) and 6 rain events in the Maroni catchment (Négrel and Lachassagne 2000) are shown together with the Global Meteoric Water Line (GMWL: Craig, 1961); see text for origin of additional data. The big cross indicates the mean weighted rain input. In the extended view (b), the regression line and error bar envelope are indicated for the LMWL.

Fig. 3. Relations entre δ^2H et $\delta^{18}O$ (‰ vs SMOW Standard Mean Ocean Water) dans les eaux de surface et souterraines de Guyane (a). Les données des pluies, e.g. droite météorique locale (LMWL, i.e. 10 échantillons mensuels intégrés, 3 pluies individuelles à Cayenne [Négrel et al., 1997] et 6 pluies individuelles dans le bassin versant du Maroni [Négrel and Lachassagne 2000]), sont illustrées avec la droite météorique mondiale (Global Meteoric Water Line GMWL: Craig, 1961). Les croix sur le schéma indiquent les valeurs moyennes pondérées des pluies. Dans la vue étendue (b), sont indiquées la droitre de régression et les enveloppes d'incertitude pour la droite météorique locale LMWL.

recharge occurring during May to July. During this period, the rainfall was 943.3 mm, (52.7% of the total annual rainfall) and the mean weighted rain input led to $\delta^{18}O$ and $\delta^{2}H$ signatures of around −4.24 and −20.89‰, respectively. This period of rain and thus recharge may explain the most negative δ-values in the groundwater samples. This suggests different stages of groundwater recharge with isotope signatures in close connection with the range in rainwater.

4.3. $^{87}Sr/^{86}Sr$ as a proxy of weathering processes

Sr isotope studies of rivers and lakes have shown that variations in $^{87}Sr/^{86}Sr$ and Sr contents are caused by mixing waters with different $^{87}Sr/^{86}Sr$ ratios and Sr contents, each of them reflecting water-rock interaction with different rock types (Chung et al., 2009; Grove et al., 2003; Oliver et al., 2003).

All the surface- and groundwater samples from French Guiana are plotted in a $^{87}Sr/^{86}Sr$ versus 1/Sr diagram (Fig. 4a), which is classically used to evaluate two-component mixing and end-member water compositions. This figure indicates the existence of at least three end-members. The surface waters from the Maroni catchment, reported from Négrel and Lachassagne, 2000, plot along the mixing trend between the end-members corresponding to the drainage of the Unit P metavolcanic rocks (low $^{87}Sr/^{86}Sr$ ratio, highest [Sr]) and that of the Unit S metasedimentary lithology (highest $^{87}Sr/^{86}Sr$ ratio, intermediate [Sr]). The low $^{87}Sr/^{86}Sr$ ratio would reflect the weathering of rocks such as basalt and amphibolite that are known to impart a low $^{87}Sr/^{86}Sr$ ratio to the waters (Dessert et al., 2001; Louvat and Allègre, 1997) while the high $^{87}Sr/^{86}Sr$ ratio would be related to the weathering of schists and micaschists, which deliver higher $^{87}Sr/^{86}Sr$ ratios to the water (Aubert et al., 2002). This compares to the results obtained on rivers draining "undifferentiated Proterozoic rocks" of the Guyana Shield (Edmond et al., 1995), which also lie on the mixing trend between the S and P end-members. The third end-member (intermediate $^{87}Sr/^{86}Sr$ ratio, low [Sr]) could correspond to the drainage of plutonic granitoid intrusions (δη). In the Maroni catchment, the shift of some surface waters to the right of the mixing trend between S and P end-members could reflect the input into the main stream of tributaries draining weathered granitoids. This is also illustrated by some rivers from the GWA/alt-sed (Négrel et al., 2002) that plot in the field δη in the Fig. 4a. Some ground waters from the same area plot very close to the mixing trend between S and P end-members but most of them plot with a low $^{87}Sr/^{86}Sr$ ratio, reflecting the influence of the drainage of volcanic rocks of the Lower Paramaca (Unit P). It is worth noting that some points of groundwater are shifted with a higher 1/Sr ratio agreeing with the rainwater samples. Therefore, it may be concluded that the shift reflects a large rainwater input for the Sr budget compared to the Sr released by water-rock interaction.

The GWA/bas groundwaters lie on the straight line corresponding to a mixing between waters that have interacted with rocks from Unit P and S. Most ground waters display the lowest $^{87}Sr/^{86}Sr$ ratio, reflecting the interaction with rocks having a low Sr isotopic ratio. However, the location of the deep groundwaters from Grand Santi (F1, F2) is not consistent with an interaction with volcanic rocks of the Unit P because the boreholes were drilled within granitoids. One way to explain the similarity between the drainage of volcanic rocks (Unit P) and ground waters that have interacted with granitoids is

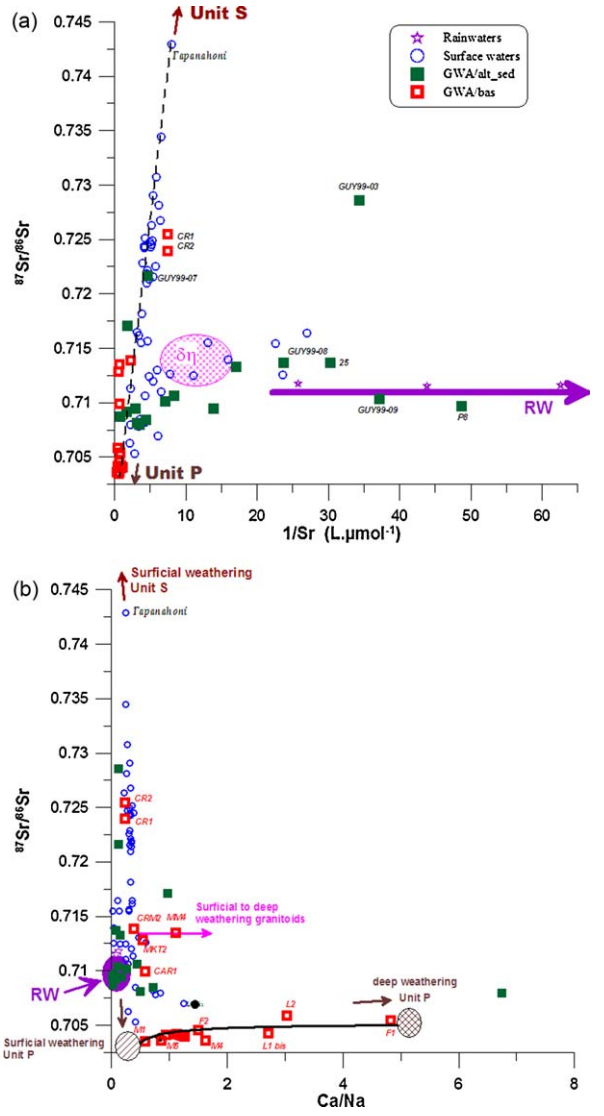

Fig. 4. Relationship between (a) $^{87}Sr/^{86}Sr$ ratios and 1/Sr and (b) $^{87}Sr/^{86}Sr$ ratios and Ca/Na ratios in surface- and groundwaters collected from French Guiana. Rainwater data are from Négrel et al. (1997) and surface water data are from Négrel and Lachassagne (2000). **Unit S**: schists, micaschists, quartzites, conglomerates, metagrauwackes, metasiltites. **Unit P**: meta-volcanic rocks (basalt, amphibolite) and rare sediments. δη: gabbro-dioritic intrusions, granite and granodiorite.

Fig. 4. Relation entre (a) rapports $^{87}Sr/^{86}Sr$ et 1/Sr et (b) rapports $^{87}Sr/^{86}Sr$ et rapports Ca/Na dans les eaux de surface et souterraines de Guyane. Les données des eaux de pluie sont extraites de Négrel et al. (1997) ; celles des eaux de surface sont extraites de Négrel et Lachassagne (2000). **Unit S** : schistes, micaschistes, quartzites, conglomérats, métagrauwackes, métasiltites. **Unit P** : roches méta-volcaniques (basalte, amphibolite) et rares sédiments. δη : intrusions gabbro-dioritiques, granite et granodiorite.

to consider that the latter are influenced by the weathering of low Rb-rich Sr phases, which would impart a low $^{87}Sr/^{86}Sr$ ratio to the waters. Weathering of low Rb-rich Sr phases and more constraints on the $^{87}Sr/^{86}Sr$ ratio variations may be tested through a diagram $^{87}Sr/^{86}Sr$ versus Ca/Na ratio (Fig. 4b). The use of a cation ratio rather than absolute concentrations alone, avoids variations due to dilution or concentration effects (BenOthmann et al., 1997; Chung et al., 2009). As previously detailed, when Ca is compared to Cl content (Fig. 2b), all groundwaters are indicative of a Ca^{2+} excess, more marked in the ground waters from the basement, as well as for Mg, while the Na enrichment is less. Thus, Ca/Na appears to be a good indicator of weathering processes in waters from French Guiana. The surface water from the Maroni catchment does not define a clear hyperbola that binary mixing should lead to (Langmuir et al., 1978). They appear rather to be scattered along a main trend showing a large fluctuation in the $^{87}Sr/^{86}Sr$ ratio with a weak Ca/Na range. This makes possible to define a first water-rock interaction process that corresponds to surficial weathering of unit P and S. Surficial weathering of Unit S shows a larger $^{87}Sr/^{86}Sr$ ratio without changes in the Ca/Na ratio. Rainwater field (RW in Fig. 4) shows a low Ca/Na ratio and a $^{87}Sr/^{86}Sr$ ratio around 0.710. Two other trends can be defined with a weak fluctuation in the $^{87}Sr/^{86}Sr$ ratio within a change of the Ca/Na ratio. The first trend corresponds to a water-rock interaction process from the surficial to the deep weathering of granitoids. The deeper weathering of granitoids reflected in this trend implies that the weathering of Ca-bearing phases (e.g. plagioclases and/or calcite, Pett-Ridge et al., 2009) is greater in sample MM4 than in sample CRM2. The second trend corresponds to a water-rock interaction process from the surficial to the deep weathering of the unit P with a weak fluctuation of the $^{87}Sr/^{86}Sr$ ratio (around 0.704) associated with a large increase in the Ca/Na ratio. As for the first water-rock interaction processes, the shift towards a relatively high Ca/Na ratios can be explained by more extensive weathering of Ca-bearing phases with a low $^{87}Sr/^{86}Sr$ ratio, such as plagioclase and/or calcite. High Ca/Na ratios generally relate to carbonate weathering (Gaillardet et al., 1997), which is also accompanied by increase in the Mg/Sr and Ca/Sr ratios (Rengarajan et al., 2009). The increase in the Ca/Na ratios during the weathering of the unit P is accompanied by an increase of the Ca/Sr ratios (up to 500) not withstanding that this value is the lowermost value of carbonate weathering (Meybeck, 1986). On the other hand, large Ca/Na ratios were observed during basalt weathering (up to 3, Dessert et al., 2001; Raiber et al., 2009; Rengarajan et al., 2009). Such large Ca/Na ratios were accompanied by Ca/Sr ratio around 500 (Dessert et al., 2001). Thus, we can conclude that the trend in the GWA/bas ground waters from the unit P may reflect a more intense weathering of Ca-bearing phases like plagioclases as no evidence of calcite has been reported in basalts.

Using the $^{87}Sr/^{86}Sr$ and Ca/Na ratios of the extreme samples of the surficial and deep weathering of the unit P, which can be considered as end-members, a mixing line was calculated and reported in Fig. 4b. The first end-member corresponds to the surficial weathering with a $^{87}Sr/^{86}Sr$ and Ca/Na ratios of around 0.703 and 0.4. The latter represents the value classically used for the weathering of silicate rocks (Gaillardet et al., 1997; Louvat and Allègre, 1997; Rengarajan et al., 2009). The second end-member shows a slightly higher $^{87}Sr/^{86}Sr$ ratio (i.e., 0.705) and a greater Ca/Na ratio (i.e., 5). The calculation led to a divergence from the surficial weathering end-member of around 10% for F5, 25% for F2 and M4 and 50–60% for L1bis and L2.

4.4. Nd contents and Nd isotopes: implications for water–rock interactions

Since the development of the method by ICP-MS to determine the dissolved REE concentrations (Johannesson and Lyons, 1995; Stetzenbach et al., 1994), many studies deal with the behaviour of the REE in continental waters (Andersson et al., 2001; Gaillardet et al., 1997; Janssen and Verweij, 2003; Viers et al., 2000 and references therein) but, in contrast, neodymium isotopes have not been extensively used in hydrogeological studies. Some data are available on the compositions of river water (Andersson et al., 2001; Goldstein and Jacobsen, 1987; Steinmann and Stille, 2006; Tricca et al., 1999) and very little information is available for saline waters (Négrel, 2006) and ground waters (Tricca et al., 1999; Viers and Wasserburg, 2004). The contents of Sm and Nd, as well as for the other dissolved REEs vary greatly. The dissolved Nd content in the surface waters varies from 20 to 102 ng/L with a low TDS (10–20 mg/L), in agreement with values reported by other studies (Amazon: Gaillardet et al., 1997; Cameroon: Viers et al., 2000; Viers and Wasserburg, 2004), but broadly independent of other parameters such as total dissolved solids and pH. In the groundwater from the GWA/alt-sed, the dissolved Nd content varies from 39 to 752 ng/L together with a broad range in the TDS (10 up to 166 mg/L). In the GWA/bas groundwater, the dissolved Nd contents are lower and vary from 3 to 63 ng/L with TDS values ranging from 46 to 218 mg/L. These ranges agree with other studies in groundwater (Oliva et al., 1999; Viers and Wasserburg, 2004). As usually stated in terrestrial surface processes and in granite-gneiss rocks, Sm displays similar behaviour to Nd ($Nd = 4.9 \times Sm + 6.5$, $r^2 = 0.98$, $n = 30$), because of the similarity in their physical and chemical properties (Gaillardet et al., 1997; Goldstein and Jacobsen, 1987; Viers and Wasserburg, 2004). The isotopic composition of dissolved Nd in surface and ground waters from French Guiana ranges from $^{143}Nd/^{144}Nd = 0.511377 \pm 9 \times 10^{-6}$ to $0.512162 \pm 8 \times 10^{-6}$ corresponding to a range of $\varepsilon Nd(0)$ from −9.2 to −24.6. The lowest $\varepsilon Nd(0)$ are observed in the GWA/alt-sed groundwater whereas the highest are for the GWA/bas groundwater. The small differences between $\varepsilon Nd(0)$ values for both the dissolved and suspended phases found within the same rivers suggests that the Nd isotopic composition can be used as an indicator of the weathered parent rock (Goldstein and Jacobsen, 1987, 1988; Tricca et al., 1999). Mixing processes and water–rock interaction have both contributed to the observed $\varepsilon Nd(0)$ (Négrel et al., 2001).

The similarity between the $^{143}Nd/^{144}Nd$ ratios in waters and related bedrock can be postulated now according to the recent works by Aubert et al. (2001). Comparing the Nd and Sr isotopic composition in minerals and waters, they

demonstrated that the Sr and Nd isotopic characteristics of the major mineral phases of a granite clearly shows the strong influence of plagioclase and phosphate minerals (e.g. apatite) on the isotopic composition of the spring and stream waters. This was confirmed on other granite massif (France) by Négrel (2006). Thus, comparison of the εNd(0) values with the corresponding Sm/Nd ratios (e.g. $^{147}Sm/^{144}Nd$ ratios represented with the propagate errors) yields more information about the origin of the REE in the waters from French Guiana (Fig. 5). With the exception of the samples GUY99-11 and F1, they are positively correlated ($\varepsilon Nd(0) = -43.3 + 233.8 \times {}^{147}Sm/^{144}Nd$; $r^2 = 0.64$; $n = 16$) with low $^{147}Sm/^{144}Nd$ ratios for the river water and rather high ratios for the ground waters.

Most of the ground waters have $^{147}Sm/^{144}Nd$ ratios significantly higher than the average continental crust value of 0.105 (Allègre and Lewin, 1989). The εNd(0) versus the $^{147}Sm/^{144}Nd$ ratio in the surface water and GWA/bas groundwater, illustrated in Fig. 5, are consistent with that of the parent rocks (Delor et al., 2001; Gruau et al., 1985). If the εNd(0) is mostly controlled by the weathering of plagioclase and phosphate phases, as suggested by Aubert et al. (2001) and Négrel (2006), they should be shifted towards higher εNd(0) and Sm/Nd ratios and thus would plot on the right of the parent rocks field, which is not observed. The εNd(0) versus the $^{147}Sm/^{144}Nd$ ratio for the groundwater from the GWA/alt-sed plot between the values measured in the parent rocks and that of suspended matter from the Amazon Basin (Allègre et al., 1996; Goldstein et al., 1984). This suggests for some groundwater a possible influence of sedimentary deposits in the coastal area that originate from the Amazon. The other groundwater from the same area agrees with the field of parent rocks, suggesting that Nd originates from the weathering of the bedrock.

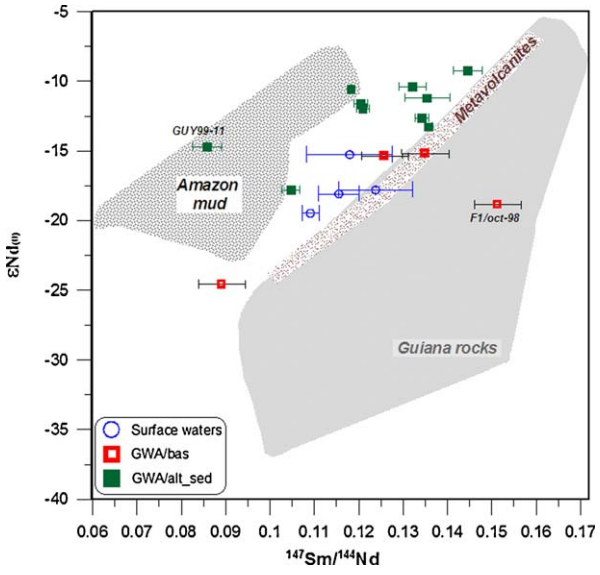

Fig. 5. Plot of εNd(0) versus $^{147}Sm/^{144}Nd$ in surface- and groundwaters collected from French Guiana. Bedrock whole rocks εNd(0) fields are from Deckart et al. (2005), Delor et al. (2001), and Gruau et al. (1985) and the Amazon suspended matter data are from Allègre et al. (1996).

Fig. 5. Diagramme entre εNd(0) versus $^{147}Sm/^{144}Nd$ dans les eaux de surface et souterraines de Guyane. Les données des roches totales sont extraites de Deckart et al. (2005), Delor et al. (2001) et Gruau et al. (1985). Les données des matières en suspension de l'Amazone sont extraites d'Allègre et al. (1996).

5. Summary and perspectives

We report the dissolved concentrations of major and trace elements, stable isotopes (O and D), strontium ($^{87}Sr/^{86}Sr$) and neodymium isotopes ($^{143}Nd/^{144}Nd$) in ground waters and surface waters in French Guiana. Groundwater samples were collected from:

- shallow drill holes in this coastal area, which is the only densely populated area in French Guiana;
- deeper wells in the basement from which groundwater is pumped from bedrock fractures.

Major cations show excess due to water-rock interaction. Comparing $\delta^{18}O$ and $\delta^{2}H$ reveals that most ground waters agree with both local and global meteoric water lines without evaporation impacts. The $^{87}Sr/^{86}Sr$ ratios indicate the existence of at least three end-members that corresponds respectively to the drainage of metavolcanic rocks, meta-sedimentary lithology and plutonic granitoid intrusions. The $^{87}Sr/^{86}Sr$ and Ca/Na ratios yield evidence of increase in the weathering of metavolcanic rocks with the larger divergence between surficial and deep weathering of about 60%. The εNd(0) in some ground waters reveals a possible influence of sedimentary deposits in the coastal area that originate from the Amazon and on the other hand, some groundwaters plot in agreement with the field of parent rocks, suggesting that Nd originates from the weathering of the bedrock. This geochemical and isotopic approach to the groundwater in French Guiana has allowed the origin and complex relationships between the different compartments of the hard-rock aquifers to be more clearly defined.

Acknowledgements

This work was funded by the BRGM Research Division. Chemical and isotopic analyses were performed in the Geochemistry Laboratory of the BRGM, France. We thank the two anonymous reviewers for providing critical comments that improved this manuscript. We are grateful to Dr. H.M. Kluijver for proofreading and editing the English text.

References

Allègre, C.J., Lewin, E., 1989. Chemical structure and history of the Earth: evidence from global non-linear inversion of isotopic data in a three-box-model. Earth Planet. Sci. Lett. 96, 61–88.

Allègre, C.J., Dupré, B., Négrel, P., Gaillardet, J., 1996. Sr-Nd-Pb isotopes systematics in Amazon and Congo River systems. Constraints about erosion processes. Chem. Geol. 131, 93–112.

Andersson, P.S., Dahlqvist, R., Ingri, J., Gustafsson, Ö., 2001. The isotopic composition of Nd in a boreal river: a reflection of selective weathering and colloidal transport. Geochim. Cosmochim. Acta 65, 521–527.

Aubert, D., Stille, P., Probst, A., 2001. REE fractionation during granite weathering and removal by waters and suspended loads: Sr and Nd isotopic evidence. Geochim. Cosmochim. Acta 65, 387–406.

Aubert, D., Probst, A., Stille, P., Viville, D., 2002. Evidence of hydrological control of Sr behavior in stream water (Strengbach catchment, Vosges mountains, France). Appl. Geochem. 17, 285–300.

Auken, E., Violette, S., d'Ozouville, N., Deffontaines, B., Sorensen, K., Viezzoli, A., de Marsily, G., 2009. An integrated study of the hydrogeology of volcanic islands using airborne transient electromagnetic: application in the Galapagos Archipelago. C. R. Geoscience 341, 899–907.

BenOthmann, D., Luck, J.M., Tournoud, M.G., 1997. Geochemistry and water dynamics: application to short time-scale flood phenomena in a small Mediterranean catchment. I. Alkalis, alkali-earth and Sr isotopes. Chem. Geol. 140, 9–28.

Boronina, A., Balderer, W., Renard, P., Stichler, W., 2005. Study of stable isotopes in the Kouris catchment (Cyprus) for the description of the regional groundwater flow. J. Hydrol. 308, 214–226.

Chung, C.H., You, C.F., Chu, H.Y., 2009. Weathering sources in the Gaoping (Kaoping) river catchments, southwestern Taiwan: insights from major elements, Sr isotopes, and rare earth elements. J. Marine Syst. 76, 433–443.

Craig, H., 1961. Isotopic variations in meteoric water. Science 133, 1702–1703.

Deckart, K., Bertrand, H., Liégeois, J.P., 2005. Geochemistry and Sr, Nd, Pb isotopic composition of the Central Atlantic Magmatic Province (CAMP) in Guyana and Guinea. Lithos 82, 289–314.

Delor, C., Egal, E., Lahondere, D., Marteau, P., 2001. Carte géologique de la Guyane, 1/500,000, 2ed, BRGM eds.

Dessert, C., Dupré, B., François, L.M., Schott, J., Gaillardet, J., Chakrapani, G., Bajpai, S., 2001. Erosion of Deccan Traps determined by river geochemistry: impact on the global climate and the $^{87}Sr/^{86}Sr$ ratio of seawater. Earth Planet. Sci. Lett. 188, 459–474.

Driscoll, N.W., Karner, G.D., 1994. Flexural deformation due to Amazon fan loading: a feedback mechanism affecting sediment delivery to margins. Geology 22, 1015–1018.

Edmond, J.M., Palmer, M.R., Measures, C.I., Grant, B., Stallard, R.F., 1995. The fluvial geochemistry and denudation rate of the Guayana shield in Venezuela. Geochim. Cosmochim. Acta 59 (16), 3301–3325.

Freyssinet, P., Farah, A.S., 2000. Geochemical mass balance and weathering rates of ultramafic schists in Amazonia. Chem. Geol. 170, 133–151.

Gaillardet, J., Dupré, B., Allègre, C.J., Négrel, P., 1997. Chemical and physical denudation in the Amazon river basin. Chem. Geol. 142, 141–173.

Goldstein, S.J., Jacobsen, S.B., 1987. The Nd and Sr Isotopic systematics of river-water dissolved material: implications for the sources of Nd and Sr in seawater. Chem. Geol. 66, 245–272.

Goldstein, S.J., Jacobsen, S.B., 1988. Nd and Sr isotopic systematics of river water suspended material: implications for crustal evolution. Earth Planet. Sci. Lett. 87, 249–265.

Goldstein, S.L., O'Nions, R.K., Hamilton, P.J., 1984. A Sm-Nd isotopic study of atmospheric dusts and particulates from major river systems Earth Planet. Sci. Lett. 70, 221–236.

Grove, M.J., Baker, P.A., Cross, S.L., Rigsby, C.A., Seltzer, G.O., 2003. Application of strontium isotopes to understanding the hydrology and paleohydrology of the Altiplano, Bolivia–Peru. Palaeogeogr. Palaeoclimatol. Palaeoecol. 194, 281–297.

Gruau, G., Martin, H., Leveque, B., Capdevilla, R., Marot, A., 1985. Rb-Sr and Sm-Nd geochronology of Lower Proterozoic granite-greenstone terrains in French Guiana, South America. Precambrian Res. 30, 63–80.

Janssen, R.P.T., Verweij, W., 2003. Geochemistry of some rare earth elements in groundwater, Vierlingsbeek, The Netherlands. Water Res. 37, 1320–1350.

Johannesson, K.H., Lyons, W.B., 1995. Rare earth element geochemistry of Colour Lake, an acidic freshwater lake on Axel Heiberg Island, Nothwest Territories, Canada. Chem. Geol. 119, 209–223.

Kendall, C., McDonnell, J.J., 1998. Isotope Tracers in Catchment Hydrology. Elsevier, 839 p

Langmuir, C.H., Vocke, R.D., Hanson, G.N., Hart, S.R., 1978. A general mixing equation with application to Icelandic basalts. Earth Planet. Sci. Lett. 37, 380–392.

Louvat, P., Allègre, C.J., 1997. Present denudation rates on the island of Reunion determined by river geochemistry: basalt weathering and mass budget between chemical and mechanical erosions. Geochim. Cosmochim. Acta 61, 3645–3669.

Meybeck, M., 1986. Composition chimique des ruisseaux non pollués de France. Sci. Geol. Bull. 39, 3–77.

Négrel, P., 2006. Water-granite interaction: clues from strontium, neodymium and rare earth elements in saprolite, sediments, soils, surface and mineralized waters. Appl. Geochem. 21, 1432–1454.

Négrel, P., Lachassagne, P., 2000. Geochemistry of the Maroni River (French Guyana) during low water stage: implications for water rock interaction and groundwater characteristics. J. Hydrol. 237, 212–233.

Négrel, P., Lachassagne, P., Laporte, P., 1997. Caractérisation chimique et isotopique des pluies de Cayenne (Guyane Francaise). C.R. Acad. Sci. Paris, Ser. IIa 324, 379–386.

Négrel, Ph., Casanova, J., Aranyossy, J.F., 2001. Strontium isotope systematics used to decipher the origin of groundwaters sampled from granitoids: the Vienne case (France). Chem. Geol. 177, 287–308.

Négrel, P., Petelet-Giraud, E., Casanova, J., Kloppmann, W., 2002. Boron isotope signatures in the coastal groundwaters of French Guiana. Water Resour. Res., doi:10.1029/2002WR001299 (Art. No. 1262 cited November 2002)http://www.agu.org.

Oliva, P., Viers, J., Dupré, B., Fortuné, J.P., Martin, F., Braun, J.J., Nahon, D., Robain H, 1999. The effect of organic matter on chemical weathering: study of a small tropical watershed: Nsimi-Zoétélé site, Cameroon. Geochim. Cosmochim. Acta 63, 4013–4035.

Oliver, L., Harris, N., Bickle, M., Chapman, H., Dise, N., Horstwood, M., 2003. Silicate weathering rates decoupled from the $^{87}Sr/^{86}Sr$ ratio of the dissolved load during Himalayan erosion. Chem. Geol. 201, 119–139.

Pett-Ridge, J.C., Derry, L.A., Kurtz, A.C., 2009. Sr isotopes as a tracer of weathering processes and dust inputs in a tropical granitoid watershed, Luquillo Mountains, Puerto Rico. Geochim. Cosmochim. Acta 73, 25–43.

Raiber, M., Webb, J.A., Bennetts DA, 2009. Strontium isotopes as tracers to delineate aquifer interactions and the influence of rainfall in the basalt plains of southeastern Australia. J. Hydrol. 367, 188–199.

Rengarajan, R., Singh, S.K., Sarin, M.M., Krishnaswami, S., 2009. Strontium isotopes and major ion chemistry in the Chambal River system. India: Implications to silicate erosion rates of the Ganga. Chem. Geol. 260, 87–101.

Sailhac, P., Bano, M., Behaegel, M., Girard, J.-F., Falgàs Para, E., Ledo, J., Marquis, G., Matthey, P.-D., Ortega-Ramírez, J., 2009. Characterizing the vadose zone and a perched aquifer near the Vosges ridge at the La Soutte experimental site, Obernai, France. C. R. Geoscience 341, 818–830.

Steinmann, M., Stille, P., 2006. Rare earth element transport and fractionation in small streams of a mixed basaltic–granitic catchment basin (Massif Central France). J. Geochem. Explor. 88, 336–340.

Stetzenbach, K.J., Amano, M., Kreamer, D.K., Hodge, V.F., 1994. Testing the limits of ICP-MS: determination of trace elements in groundwater at the part-per-trillion level. Groundwater 32, 976–985.

Tricca, A., Stille, P., Steinman, M., Kiefel, B., Samuel, J., Eikenberg, J., 1999. Rare earth elements and Sr and Nd isotopic compositions of dissolved and suspended loads from small river systems in the Vosges mountains (France), the river Rhine and groundwater. Chem. Geol. 160, 139–158.

Viers, J., Wasserburg, G.J., 2004. Behavior of Sm and Nd in a lateritic soil profile. Geochim. Cosmochim. Acta 68, 2043–2054.

Viers, J., Dupré, B., Braun, J.J., Deberdt, S., Angeletti, B., Ngoupayou, J.N., Michard, A., 2000. Major and trace element abundances, and strontium isotopes in the Nyong basin rivers (Cameroon): constraints on chemical weathering processes and elements transport mechanisms in humid tropical environments. Chem. Geol. 169, 211–241.